

Selective-Resonance-Based Quantum Entangling Operation on Qubits in Circuit QED

Ming Hua and Fu-Guo Deng*

*Department of Physics, Applied Optics Beijing Area Major Laboratory,
Beijing Normal University, Beijing 100875, China*

(Dated: January 2, 2022)

We present a fast quantum entangling operation on superconducting qubits assisted by a resonator in the quasi-dispersive regime with a new effect — the selective resonance coming from the amplified qubit-state-dependent resonator transition frequency and the tunable period relation between a wanted quantum Rabi oscillation and an unwanted one. This operation does not require any kind of drive fields and the interaction between qubits. More interestingly, the non-computational third excitation states of the charge qubits can play an important role in shortening largely the operation time of the entangling gates. All those features provide an efficient way to realize much faster quantum entangling gates on superconducting qubits than previous proposals.

PACS numbers: 03.67.Lx, 03.67.Bg, 85.25.Dq, 42.50.Pq

Quantum information and quantum computation [1] has attracted much attention. Constructing universal quantum gates and generating multipartite entanglement are two key tasks in this topic, especially those based on superconducting qubits [2–5]. Circuit quantum electrodynamics (QED), combining the method of cavity QED and superconducting circuits, has been widely studied for quantum information processing [6–15], because of both its long-coherence time and its good scalability. Since the first physical mode was proposed by Yale group [6], circuit QED has been used for resolving photon number states in a superconducting circuit [16], constructing the quantum non-demolition detector for measuring the number of photons inside a high-quality-factor microwave cavity on a chip [17], simulating the basic interaction between an atom and a cavity even in the ultrastrong coupling regime [18], and realizing the quantum information processing between superconducting qubits or between microwave photons [7–10, 19–21].

Circuit QED can also provide an effective control on superconducting qubits in some important regimes by choosing the coupling strength between a qubit and a cavity [16], such as the dispersive regime ($|\frac{g_i^j}{\Delta_i^j}| \ll 1$) [22, 23], the quasi-dispersive regime ($0.1 < |\frac{g_i^j}{\Delta_i^j}| < 1$) [16, 20], the resonant regime ($|\frac{g_i^j}{\Delta_i^j}| > 1$) [19, 24], and even the ultrastrong coupling regime ($0.1 < |\frac{g_i^j}{\omega_{r_j}}| < 1$) [18, 25]. Here g_i^j is the coupling strength between the qubit q_i and the resonator R_j . ω_{r_j} and ω_i are the frequencies of R_j and q_i , respectively. $\Delta_i^j = \omega_{r_j} - \omega_i$. Aiming to find an effective high-fidelity quantum entangling operation on superconducting qubits in circuit QED with shorter operation time, we pay close attention to two of the critical characters of the dispersive regime in cavity QED [19]: the qubit-state-dependent (QSD) transi-

tion on a cavity [26, 27] and the number-state-dependent (NSD) transition on a qubit [20, 28]. By increasing the coupling strength between a qubit and a cavity, the QSD resonator transition frequency and the NSD qubit transition frequency can be amplified effectively. The amplified NSD qubit transition frequency in circuit QED has been studied by Strauch, Jacobs, and Simmonds in 2010, and they gave an interesting effect — a selective rotation [20] with a drive field, which can be used to generate the entanglement between two microwave photons effectively.

In this paper, we investigate the effect from the amplified QSD resonator transition frequency in the quasi-dispersive regime in circuit QED and its application in quantum entangling operation and entanglement generation for superconducting qubits. We use charge superconducting qubits to describe our results by taking the influence from the non-computational third excitation states of the qubits into account.

The Hamiltonian of a superconducting qubit coupled to a resonator can be described as ($\hbar = 1$),

$$H = \omega_r a^+ a + \omega \sigma^+ \sigma^- + g (a + a^+) (\sigma^- + \sigma^+), \quad (1)$$

where $\sigma^+ = |1\rangle\langle 0|$ and a^+ are the creation operators of a qubit q and a resonator R , respectively. When we consider the dispersive regime, after making rotating-wave approximation and a unitary transformation $U = \exp[\frac{g}{\Delta} (a\sigma^+ - a^+\sigma^-)]$ on the Hamiltonian H , we can get

$$UHU^+ \approx \omega_r a^+ a + \frac{1}{2} \left[\omega_q + \frac{g^2}{\Delta} (2a^+ a + 1) \right] \sigma_z \quad (2)$$

or

$$UHU^+ \approx \left(\omega_r + \frac{g^2}{\Delta} \sigma_z \right) a^+ a + \frac{1}{2} \left(\omega_q + \frac{g^2}{\Delta} \right) \sigma_z. \quad (3)$$

Eq.(2) means the NSD qubit transition and Eq.(3) means the QSD resonator transition, shown in Fig.1(a) and (b), respectively.

The NSD qubit transition comes from the effect that the transition frequency of the qubit depends on the photon number in the resonator with $\omega'_q = \omega_q + \frac{g^2}{\Delta} (2a^+ a + 1)$,

*Corresponding author: fgdeng@bnu.edu.cn

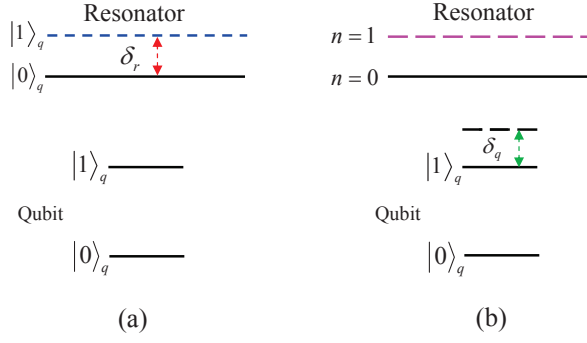


FIG. 1: (color online) (a) The qubit-state-dependent resonator transition, which means the frequency shift of the resonator transition δ_r arises from the state ($|0\rangle_q$ or $|1\rangle_q$) of the qubit. (b) The number-state-dependent qubit transition, which means the frequency shift δ_q takes place on the qubit due to the photon number $n = 1$ or 0 in the resonator in the dispersive regime.

where ω'_q is the frequency of the qubit after the NSD effect. The QSD resonator transition is the effect that the transition frequency of the resonator depends on the state of the qubit with $\omega'_r = \omega_r + \sigma_z \frac{g^2}{\Delta}$. Here ω'_r is the frequency of the resonator after the QSD effect. From Eq.(2) and Eq.(3), one can see that the NSD qubit transition frequency and the QSD resonator transition frequency can be amplified effectively when $\frac{g^2}{\Delta}$ is large enough, which means the number of photons in the cavity can make a large shift on the transition frequency of the qubit and the qubit in different states will also make a large shift on the transition frequency of the resonator. The NSD qubit transition in the quasi-dispersive regime was used as an effective method to realize entanglement and quantum gates between microwave photons [16, 17, 20]. In fact, the QSD resonator transition frequency can also be amplified in the quasi-dispersive regime effectively.

In order to show the influence on the resonance between a qubit and a resonator by the amplified QSD resonator transition frequency, let us consider the case that two perfect qubits couple to a resonator (i.e., R_a) with the Hamiltonian

$$H_{2q} = \omega_{r_a} a^\dagger a + \omega_1 \sigma_1^+ \sigma_1^- + \omega_2 \sigma_2^+ \sigma_2^- + g_1 (a^\dagger + a) \otimes (\sigma_1^+ + \sigma_1^-) + g_2 (a^\dagger + a) (\sigma_2^+ + \sigma_2^-) \quad (4)$$

in which we neglect the direct interaction between the two qubits (i.e., q_1 and q_2), shown in Fig.2. Here $\sigma_i^+ = |1\rangle_i \langle 0|$ is the creation operator of q_i ($i = 1, 2$). g_i is the coupling strength between q_i and R_a . The parameters are chosen to make q_1 interact with R_a in the quasi-dispersive regime. That is, the transition frequency of R_a is determined by the state of q_1 . By taking a proper transition frequency of q_2 (which equals to the transition frequency of R_a when q_1 is in the state $|0\rangle_1$), one can realize the quantum Rabi oscillation (ROT) $\text{ROT}_0: |0\rangle_1 |1\rangle_2 |0\rangle_a \leftrightarrow |0\rangle_1 |0\rangle_2 |1\rangle_a$, while $\text{ROT}_1: |1\rangle_1 |1\rangle_2 |0\rangle_a \leftrightarrow |1\rangle_1 |0\rangle_2 |1\rangle_a$, while $\text{ROT}_1: |1\rangle_1 |1\rangle_2 |0\rangle_a \leftrightarrow |1\rangle_1 |0\rangle_2 |1\rangle_a$, while $\text{ROT}_1: |1\rangle_1 |1\rangle_2 |0\rangle_a \leftrightarrow |1\rangle_1 |0\rangle_2 |1\rangle_a$.

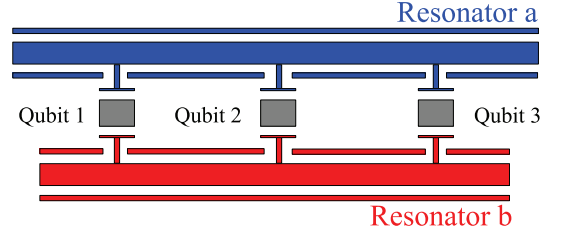


FIG. 2: (color online) Sketch of a coplanar geometry for the circuit QED with three superconducting qubits. Qubits are placed around the maxima of the electrical field amplitude of R_a and R_b (not drawn in this figure), and the distance between them is large enough so that there is no direct interaction between them. The fundamental frequencies of resonators are $\omega_{r_j}/(2\pi)$ ($j = a, b$), the frequencies of the qubits are $\omega_{q_i}/(2\pi)$ ($i = 1, 2, 3$), and they are capacitively coupled to the resonators. The coupling strengths between them are $g_j^2/(2\pi)$. We can use the control line (not drawn here) to afford the flux to tune the transition frequencies of the qubits.

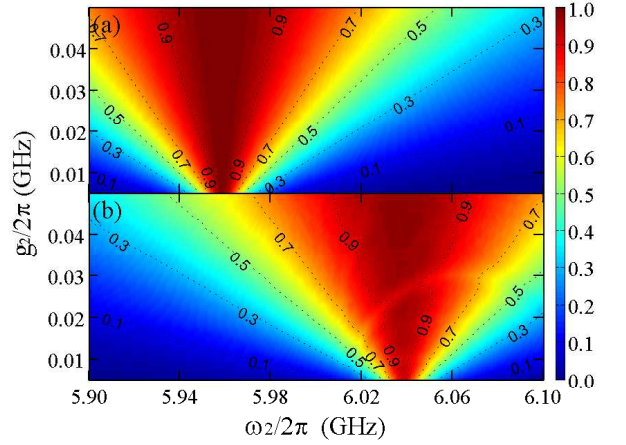


FIG. 3: (color online) Simulated outcomes for the maximum amplitude value of the expectation about the quantum Rabi oscillation varying with the coupling strength g_2 and the frequency of the second qubit ω_2 . (a) The outcomes for $\text{ROT}_0: |0\rangle_1 |1\rangle_2 |0\rangle_a \leftrightarrow |0\rangle_1 |0\rangle_2 |1\rangle_a$. (b) The outcomes for $\text{ROT}_1: |1\rangle_1 |1\rangle_2 |0\rangle_a \leftrightarrow |1\rangle_1 |0\rangle_2 |1\rangle_a$. Here the parameters of the resonator and the first qubit q_1 are taken as $\omega_a/(2\pi) = 6.0$ GHz, $\omega_{q_1}/(2\pi) = 7.0$ GHz, and $g_1/(2\pi) = 0.2$ GHz.

$|1\rangle_1 |1\rangle_2 |0\rangle_a \leftrightarrow |1\rangle_1 |0\rangle_2 |1\rangle_a$ occurs with a small probability as q_2 detunes with R_a when q_1 is in the state $|1\rangle_1$. Here the Fock state $|n\rangle_a$ represents the photon number n in R_a ($n = 0, 1$). $|0\rangle_i$ and $|1\rangle_i$ are the ground and the first excited states of q_i , respectively.

We numerically simulate the maximal expectation values (MAEVs) of ROT_0 and ROT_1 based on the Hamiltonian H_{2q} , shown in Fig. 3(a) and (b), respectively. Here, the expectation value is defined as $|\langle \psi | e^{-iH_{2q}t/\hbar} | \psi_0 \rangle|^2$. $|\psi_0\rangle$ and $|\psi\rangle$ are the initial and the final states of a quantum Rabi oscillation, respectively. The MAEV s

vary with the transition frequency ω_2 and the coupling strength g_2 . It is obvious that the amplified QSD resonator transition can generate a *selective resonance* (SR) when the coupling strength g_2 is small enough.

It is worth noticing that there is a detune between g_2 and R_a in ROT_1 , when g_2 is resonant with R_a for realizing ROT_0 with a large probability. In principle, the frequency of the quantum Rabi oscillation between a qubit and a resonator can be described as [29]

$$\Omega_n^2 = \Delta^2 + 4g^2(n+1), \quad (5)$$

where n is the number of photons in the resonator. One can see that the period of ROT_0 is different from that of ROT_1 as $\Delta = 0$ for ROT_0 and $\Delta = \delta_r$ for ROT_1 . By taking a proper parameter for g , we can tune the different period relation between these two quantum Rabi oscillations. That is, a *tunable period relation* between a wanted quantum Rabi oscillation and an unwanted one can also be obtained.

In the discussion below, we consider practical charge superconducting qubits in which there are two computational levels $|0\rangle_q$ and $|1\rangle_q$ for our selective-resonance-based entangling operation, by taking the influence from the non-computational third excitation state $|2\rangle_q$ of each charge qubit into account. When the two charge qubits q_1 and q_2 are coupled to the resonator R_a , the SR is simulated with the Hamiltonian

$$\begin{aligned} H'_{2q} = & \sum_{\substack{i=0,1,2 \\ q=1,2}} E_{i;q} |i\rangle_q \langle i| + \omega_{r_a} a^\dagger a + g_{0,1;1} (a^\dagger + a) (\sigma_{0,1;1}^+ + \sigma_{0,1;1}^-) \\ & + g_{1,2;1} (a^\dagger + a) (\sigma_{1,2;1}^+ + \sigma_{1,2;1}^-) + g_{0,1;2} (a^\dagger + a) \\ & \otimes (\sigma_{0,1;2}^+ + \sigma_{0,1;2}^-) + g_{1,2;2} (a^\dagger + a) (\sigma_{1,2;2}^+ + \sigma_{1,2;2}^-), \quad (6) \end{aligned}$$

and it is shown in Fig.4 (a). In the simulation of our SR, we choose the reasonable parameters by considering the energy level structure of a charge qubit, according to Ref. [30]. Here $\omega_{r_a}/(2\pi) = 6.0$ GHz. The transition frequency of two qubits between $|0\rangle_q \leftrightarrow |1\rangle_q$ and $|1\rangle_q \leftrightarrow |2\rangle_q$ are chosen as $\omega_{0,1;1}/(2\pi) = E_{1;1} - E_{0;1} = 5.0$ GHz, $\omega_{1,2;1}/(2\pi) = E_{2;1} - E_{1;1} = 6.2$ GHz, $\omega_{0,1;2}/(2\pi) = E_{1;2} - E_{0;2} = 6.035$ GHz, and $\omega_{1,2;2}/(2\pi) = E_{2;2} - E_{1;2} = 7.335$ GHz. Here $E_{i;q}$ is the energy for the level i of the qubit q , and $\sigma_{i,i';q}^+ \equiv |i\rangle_q \langle i'|$. $g_{i,j;q}$ is the coupling strength between the resonator R_a and the qubit q in the transition between the energy levels $|i\rangle_q$ and $|j\rangle_q$ ($i = 0, 1, j = 1, 2$, and $q = 1, 2$). For convenience, we take the coupling strengths as $g_{0,1;1}/(2\pi) = g_{1,2;1}/(2\pi) = 0.2$ GHz and $g_{0,1;2}/(2\pi) = g_{1,2;2}/(2\pi) = 0.0488$ GHz.

SR also provides us a high-fidelity quantum entangling operation on charge qubits, assisted by a resonator. This operation gives us a different way to realize the controlled-phase (c-phase) gate on the two qubits q_1 and q_2 . Although the amplitude of ROT_1 is not very small, one can see that within a period of ROT_0 , ROT_1 completes two periods accurately, which means that ROT_1 does not change the phase of the state $|1\rangle_1 |1\rangle_2 |0\rangle_a$. In detail, let us assume that q_1 is the control qubit and q_2 is the target qubit. The initial state

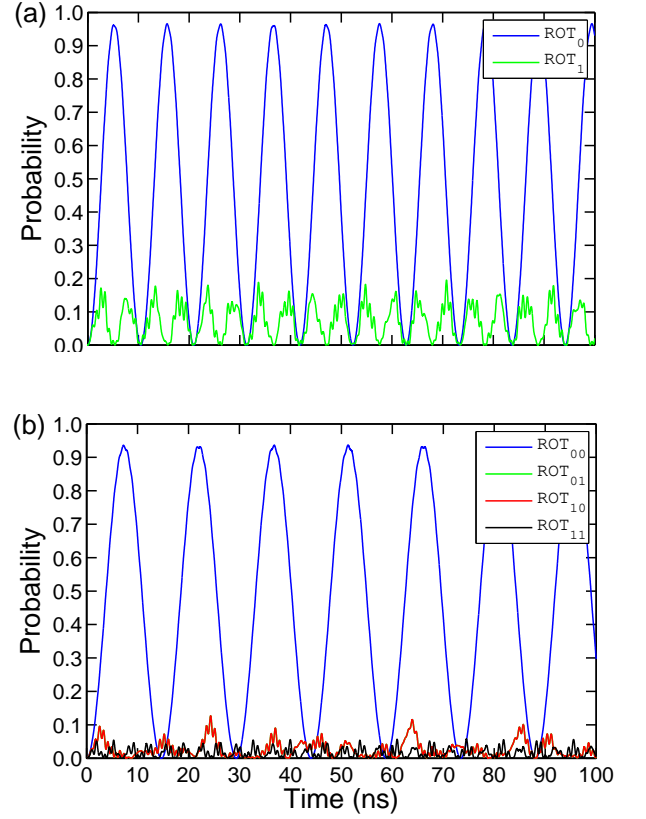


FIG. 4: (color online) (a) The probability distribution of the two quantum Rabi oscillations ROT_0 (the blue solid line) and ROT_1 (the green solid line) of two charge qubits coupled to a resonator. (b) The probability distribution of the four quantum Rabi oscillations in our cc-phase gate on a three-charge-qubit system. Here, the blue-solid, green-solid, red-dashed, and Cambridge-blue-dot-dashed lines represent the quantum Rabi oscillations ROT_{00} ($|0\rangle_1 |0\rangle_2 |1\rangle_3 |0\rangle_a \leftrightarrow |0\rangle_1 |0\rangle_2 |0\rangle_3 |1\rangle_a$), ROT_{01} ($|0\rangle_1 |1\rangle_2 |1\rangle_3 |0\rangle_a \leftrightarrow |0\rangle_1 |1\rangle_2 |0\rangle_3 |1\rangle_a$), ROT_{10} ($|1\rangle_1 |0\rangle_2 |1\rangle_3 |0\rangle_a \leftrightarrow |1\rangle_1 |0\rangle_2 |0\rangle_3 |1\rangle_a$), and ROT_{11} ($|1\rangle_1 |1\rangle_2 |1\rangle_3 |0\rangle_a \leftrightarrow |1\rangle_1 |1\rangle_2 |0\rangle_3 |1\rangle_a$), respectively.

of the system composed of q_1 , q_2 , and R_a is prepared as $|\phi\rangle_0 = \frac{1}{2}(|0\rangle_1 |0\rangle_2 + |0\rangle_1 |1\rangle_2 + |1\rangle_1 |0\rangle_2 + |1\rangle_1 |1\rangle_2) |0\rangle_a$. By exploiting the SR on ROT_0 and ROT_1 and choosing $g_{0,1;2} t = \pi$, one can get the state of the system $|\phi\rangle_1 = \frac{1}{2}(|0\rangle_1 |0\rangle_2 - |0\rangle_1 |1\rangle_2 + |1\rangle_1 |0\rangle_2 + |1\rangle_1 |1\rangle_2) |0\rangle_a$. This is just the result of a c-phase gate on q_1 and q_2 . Certainly, by choosing an appropriate transition frequency of g_2 , one also can get another c-phase gate which completes the transformation $|\phi\rangle_0 \rightarrow |\phi\rangle_2 = \frac{1}{2}(|0\rangle_1 |0\rangle_2 + |0\rangle_1 |1\rangle_2 + |1\rangle_1 |0\rangle_2 - |1\rangle_1 |1\rangle_2) |0\rangle_a$. From Fig.4(a), considering the phase error of indirect interaction between the two qubits and the detune resonance between g_2 and R_a , one can get the fidelity of these two c-phase gates are about 92% within 10.2 ns.

The quantum entangling operation based on the SR can also help us to complete a single-step controlled-controlled phase (cc-phase) quantum gate on the three

charge qubits q_1 , q_2 , and q_3 by using the system shown in Fig.2 except for the resonator R_b . Here, q_1 and q_2 act as the control qubits, and q_3 is the target qubit. The initial state of this system is prepared as $|\Phi\rangle_0 = \frac{1}{2\sqrt{2}}(|0\rangle_1|0\rangle_2|0\rangle_3 + |0\rangle_1|0\rangle_2|1\rangle_3 + |0\rangle_1|1\rangle_2|0\rangle_3 + |0\rangle_1|1\rangle_2|1\rangle_3 + |1\rangle_1|0\rangle_2|0\rangle_3 + |1\rangle_1|0\rangle_2|1\rangle_3 + |1\rangle_1|1\rangle_2|0\rangle_3 + |1\rangle_1|1\rangle_2|1\rangle_3)|0\rangle_a$. In this system, both q_1 and q_2 are in the quasi-dispersive regime with R_a , and the transition frequency of q_3 is adjusted to be equivalent to that of R_a when q_1 and q_2 are in their ground states. The QSD transition frequency on R_a becomes [22]

$$\omega'_a = \omega_a + \chi_1 \sigma_1^z + \chi_2 \sigma_2^z, \quad (7)$$

where $\chi_i = \frac{g_i}{\Delta_i}$. By choosing $g_{0,1;3}t = \pi$, one can realize ROT₀₀ (where 00 means the states of the qubits in the control position are all the ground states), that is, $|\Phi\rangle_0 \rightarrow |\Phi\rangle_1 = \frac{1}{2\sqrt{2}}(|0\rangle_1|0\rangle_2|0\rangle_3 - |0\rangle_1|0\rangle_2|1\rangle_3 + |0\rangle_1|1\rangle_2|0\rangle_3 + |0\rangle_1|1\rangle_2|1\rangle_3 + |1\rangle_1|0\rangle_2|0\rangle_3 + |1\rangle_1|0\rangle_2|1\rangle_3 + |1\rangle_1|1\rangle_2|0\rangle_3 + |1\rangle_1|1\rangle_2|1\rangle_3)|0\rangle_a$. It is just the result of a cc-phase gate on the three qubits. Fig.4(b) shows the probability distributions for the four quantum Rabi oscillations in this system. In our simulation, the parameters are chosen as: $\omega_{r_a}/(2\pi) = 6.0$ GHz, $\omega_{0,1;1}/(2\pi) = E_{1;1} - E_{0;1} = 5.0$ GHz, $\omega_{1,2;1}/(2\pi) = E_{2;1} - E_{1;1} = 6.3$ GHz, $\omega_{0,1;2}/(2\pi) = E_{1;2} - E_{0;2} = 5.0$ GHz, $\omega_{1,2;2}/(2\pi) = E_{2;2} - E_{1;2} = 6.3$ GHz, $\omega_{0,1;3}/(2\pi) = E_{1;3} - E_{0;3} = 6.068$ GHz, $\omega_{1,2;3}/(2\pi) = E_{2;3} - E_{1;3} = 7.3$ GHz, $g_{0,1;1}/(2\pi) = g_{1,2;1}/(2\pi) = 0.2$ GHz, $g_{0,1;2}/(2\pi) = g_{1,2;2}/(2\pi) = 0.2$ GHz, and $g_{0,1;3}/(2\pi) = g_{1,2;3}/(2\pi) = 0.035$ GHz. The MEAVs of unwanted quantum Rabi oscillations can be suppressed a lot, and the fidelity of this cc-phase gate reaches about 86% with 14.8 ns.

A complex three-qubit gate, such as a Fredkin gate on a three-qubit system can also be constructed with the quantum entangling operation based on the SR assisted by the two resonators R_a and R_b in a simple way, shown in Fig. 2. In this system, R_b has a different transition frequency with R_a , and q_1 couples to both R_a and R_b simultaneously in the quasi-dispersive regime. Let q_2 and q_3 resonate selectively with R_a and R_b when q_1 is in the state $|1\rangle_1$, respectively, with $g_{0,1;2}^a t = g_{0,1;3}^b t = 1.5\pi$ first (here $g_{i,j;q}^k$ is the coupling strength between the resonator k and the qubit q in the transition between the energy levels $|i\rangle_q$ and $|j\rangle_q$), and then let q_2 and q_3 be selectively resonant with R_b and R_a when q_1 is in the state $|1\rangle_1$, respectively, with $g_{0,1;3}^a t = g_{0,1;2}^b t = 0.5\pi$, a Fredkin gate can be realized.

Interestingly, our gates are significantly faster than previous proposals in the quasi-dispersive regime in circuit QED [14, 15]. For example, the operation time for a c-phase gate on two perfect superconducting qubits completed in 2012 is 110 ns with the fidelity 95% in 2012 [14]. The time for the cc-phase gate is 63 ns with the fidelity 85% [15]. By taking the influence from the third levels of the superconducting qubits into account, the operation

time of our gates is reduced largely. For example, the operation time of the c-phase gate on two perfect superconducting qubits is 22 ns with the fidelity 90%, about twice of that based on the qubits with the influence from the third levels.

Our single-step quantum entangling gates have some good features. First, they do not require any kind of drive fields, which eliminates the limit on the quality of the resonator and does not increase the temperature of circuit QED, and this factor can protect the superconducting qubit in circuit QED [12] and provide a different way to realize quantum computation. Second, they are constructed without using any kind of the interaction between qubits (such as Ising-like interaction [1] and Heisenberg-like interaction [31]), similar to the c-phase gate in Refs. [14], far different from Refs. [32, 33], and our single-step universal quantum gates can be realized on the non-nearest-neighbor qubits.

Obviously, the maximal entanglement of superconducting qubit systems can be produced effectively with our quantum entangling operation. On the other hand, the operation requires different coupling strengths for different qubits with the resonator. This is not easy to design in a realistic quantum processor. Luckily, they can be obtained by using the tunable coupling qubit, which is also necessary to realize a realistic quantum processor [34, 35]. The errors of SR mainly take place with two points. First, the non-resonance ROT can generate a phase error with $e^{i\Delta t/2}$. Second, the indirect interaction between qubits can also generate the unwanted phase error. The suitable parameters taken to suppress the complex phase error should help us to get higher fidelity gates. With the stronger coupling of control qubits, the operation time of our gates can be shortened further.

In conclusion, we have proposed a selective-resonance scheme to perform a fast quantum entangling operation for quantum logic gates on superconducting qubits. This approach has many advantages over previous works. First, our quantum entangling gates are significantly faster than previous proposals. Second, they do not require any kind of drive fields. Third, the tunable period relation between a wanted quantum Rabi oscillation and an unwanted one can shorten the operation time of the gates, besides the positive influence from the non-computational third levels of the superconducting qubits. The principle of our SR can be generalized to some other similar cavity QED systems for quantum information processing.

We would like to thank Prof. Frederick W. Strauch, Prof. Chui-Ping Yang, and Dr. Qi-Ping Su for helpful discussion. Also, we would like to thank Ming-Jie Tao for his help in calculating the probability distribution. This work is supported by the National Natural Science Foundation of China under Grant No. 11174039 and NECT-11-0031.

-
- [1] M. A. Nielsen and I. L. Chuang, *Quantum Computation and Quantum Information* (Cambridge University Press, Cambridge, England, 2000).
- [2] A. Shnirman, G. Schön, and Z. Hermon, *Phys. Rev. Lett.* **79**, 2371 (1997).
- [3] F. W. Strauch, P. R. Johnson, A. J. Dragt, C. J. Lobb, J. R. Anderson, and F.C. Wellstood, *Phys. Rev. Lett.* **91**, 16 (2003).
- [4] J. Majer, J. M. Chow, J. M. Gambetta, J. Koch, B. R. Johnson, J. A. Schreier, L. Frunzio, D. I. Schuster, A. A. Houck, A. Wallraff, A. Blais, M. H. Devoret, S. M. Girvin and R. J. Schoelkopf, *Nature (London)* **449**, 443 (2007).
- [5] S. Aldana, Y. D. Wang, and C. Bruder, *Phys. Rev. B* **84**, 134519 (2011).
- [6] A. Wallraff, D. I. Schuster, A. Blais, L. Frunzio, R. S. Huang, J. Majer, S. Kumar, S. M. Girvin, and R. J. Schoelkopf, *Nature (London)* **431**, 162 (2004).
- [7] J. Q. You and F. Nori, *Nature (London)* **474**, 589 (2011).
- [8] L. DiCarlo, J. M. Chow, J. M. Gambetta, L. S. Bishop, B. R. Johnson, D. I. Schuster, J. Majer, A. Blais, L. Frunzio, S. M. Girvin, and R. J. Schoelkopf, *Nature (London)* **460**, 240 (2009).
- [9] E. Lucero, R. Barends, Y. Chen, J. Kelly, M. Mariantoni, A. Megrant, P. O'Malley, D. Sank, A. Vainsencher, J. Wenner, T. White, Y. Yin, A. N. Cleland, and J. M. Martinis, *Nature Phys.* **8**, 719 (2012).
- [10] M. D. Reed, L. DiCarlo, S. E. Nigg, L. Sun, L. Frunzio, S. M. Girvin, and R. J. Schoelkopf, *Nature (London)* **482**, 382 (2012).
- [11] Y. X. Liu, J. Q. You, L. F. Wei, C. P. Sun, and F. Nori, *Phys. Rev. Lett.* **95**, 087001 (2005); Y. D. Wang, F. Xue, Z. Song, and C. P. Sun, *Phys. Rev. B* **76**, 174519 (2007); Y. Cao, W. Y. Huo, Q. Ai, and G. L. Long, *Phys. Rev. A* **84**, 053846 (2011).
- [12] C. Rigetti, J. M. Gambetta, S. Poletto, B. L. T. Plourde, J. M. Chow, A. D. Corcoles, J. A. Smolin, S. T. Merkel, J. R. Rozen, G. A. Keefe, M. B. Rothwell, M. B. Ketchen, and M. Steffen, *Phys. Rev. B* **86**, 100506(R) (2012).
- [13] J. M. Chow, A. D. Córcoles, J. M. Gambetta, C. Rigetti, B. R. Johnson, J. A. Smolin, J. R. Rozen, G. A. Keefe, M. B. Rothwell, M. B. Ketchen, and M. Steffen, *Phys. Rev. Lett.* **107**, 080502 (2011).
- [14] J. M. Chow, J. M. Gambetta, A. D. Córcoles, S. T. Merkel, J. A. Smolin, C. Rigetti, S. Poletto, G. A. Keefe, M. B. Rothwell, J. R. Rozen, M. B. Ketchen, and M. Steffen, *Phys. Rev. Lett.* **109**, 060501 (2012).
- [15] M. D. Reed, L. DiCarlo, S. E. Nigg, L. Sun, L. Frunzio, S. M. Girvin, and R. J. Schoelkopf, *Nature (London)* **482**, 382 (2012).
- [16] D. I. Schuster, A. A. Houck, J. A. Schreier, A. Wallraff, J. M. Gambetta, A. Blais, L. Frunzio, J. Majer, B. Johnson, M. H. Devoret, S. M. Girvin, and R. J. Schoelkopf, *Nature (London)* **445**, 515 (2007).
- [17] B. R. Johnson, M. D. Reed, A. A. Houck, D. I. Schuster, Lev S. Bishop, E. Ginossar, J. M. Gambetta, L. DiCarlo, L. Frunzio, S. M. Girvin, and R. J. Schoelkopf, *Nature Phys.* **6**, 663 (2010).
- [18] D. Ballester, G. Romero, J. J. García-Ripoll, F. Deppe, and E. Solano, *Phys. Rev. X* **2**, 021007 (2012).
- [19] F. W. Strauch, *Phys. Rev. Lett.* **109**, 210501 (2012).
- [20] F. W. Strauch, K. Jacobs, and R. W. Simmonds, *Phys. Rev. Lett.* **105**, 050501 (2010).
- [21] C. P. Yang, Q. P. Su, S. B. Zheng, and S. Han, *Phys. Rev. A* **87**, 022320 (2013).
- [22] A. Blais, J. Gambetta, A. Wallraff, D. I. Schuster, S. M. Girvin, M. H. Devoret, and R. J. Schoelkopf, *Phys. Rev. A* **75**, 032329 (2007).
- [23] C. L. Hutchison, J. M. Gambetta, A. Blais, and F. K. Wilhelm, *Canad. J. Phys.* **87**, 225 (2009).
- [24] M. Sillanpää, J. I. Park, and R. W. Simmonds, *Nature (London)* **449**, 438 (2007).
- [25] G. Romero, D. Ballester, Y. M. Wang, V. Scarani, and E. Solano, *Phys. Rev. Lett.* **108**, 120501 (2012).
- [26] S. Filipp, M. Göppl, J. M. Fink, M. Baur, R. Bianchetti, L. Steffen, and A. Wallraff, *Phys. Rev. A* **83**, 063827 (2011).
- [27] J. M. Chow, L. DiCarlo, J. M. Gambetta, A. Nunnkamp, Lev S. Bishop, L. Frunzio, M. H. Devoret, S. M. Girvin, and R. J. Schoelkopf, *Phys. Rev. A* **81**, 062325 (2010).
- [28] J. Gambetta, A. Blais, D. I. Schuster, A. Wallraff, L. Frunzio, J. Majer, M. H. Devoret, S. M. Girvin, and R. J. Schoelkopf, *Phys. Rev. A* **74**, 042318 (2006).
- [29] M. O. Scully and M. S. Zubairy, *Quantum Optics* (Cambridge University Press, Cambridge, England, 1997).
- [30] J. Koch, T. M. Yu, J. Gambetta, A. A. Houck, D. I. Schuster, J. Majer, A. Blais, M. H. Devoret, S. M. Girvin, and R. J. Schoelkopf, *Phys. Rev. A* **76**, 042319 (2007).
- [31] D. Loss and D. P. DiVincenzo, *Phys. Rev. A* **57**, 120 (1998).
- [32] A. M. Chen, S. Y. Cho, and M. D. Kim, *Phys. Rev. A* **85**, 032326 (2012).
- [33] M. R. Geller, E. J. Pritchett, A. Galiatdinov, and J. M. Martinis, *Phys. Rev. A* **81**, 012320 (2010).
- [34] R. Harris, A. J. Berkley, M. W. Johnson, P. Bunyk, S. Govorkov, M. C. Thom, S. Uchaikin, A. B. Wilson, J. Chung, E. Holtham, J. D. Biamonte, A. Yu. Smirnov, M. H. S. Amin, and A. Maassen van den Brink, *Phys. Rev. Lett.* **98**, 177001 (2007).
- [35] S. J. Srinivasan, A. J. Hoffman, J. M. Gambetta, and A. A. Houck, *Phys. Rev. Lett.* **106**, 083601 (2011).